EUROPEAN COMMISSION
JOINT RESEARCH CENTRE

Institute for the Protection and the Security of the Citizen
European Laboratory for Structural Assessment (ELSA)
I-21020 Ispra (VA) Italy

European Laboratory for Structural Assessment

SEISLINES

Experimental Investigation of the Behaviour of Undeteriorated and Deteriorated Asbestos Cement Pipes under Seismic Loads (Task 5)

Final Report

2002

EUR 20520 EN

EUROPEAN COMMISSION
JOINT RESEARCH CENTRE

Institute for the Protection and the Security of the Citizen
European Laboratory for Structural Assessment (ELSA)
I-21020 Ispra (VA) Italy

European Laboratory for Structural Assessment

SEISLINES

Experimental Investigation of the Behaviour of Undeteriorated and Deteriorated Asbestos Cement Pipes under Seismic Loads (Task 5)

Final Report

2002

EUR 20520 EN

EUROPEAN COMMISSION
JOINT RESEARCH CENTRE

Institute for the Protection and the Security of the Citizen
European Laboratory for Structural Assessment (ELSA)
I-21020 Ispra (VA) Italy

SEISLINES

Experimental Investigation of the Behaviour of Undeteriorated and Deteriorated Asbestos Cement Pipes under Seismic Loads (Task 5)

Final Report

P. Negro, D. Tirelli, J. Molina, G. Magonette, V. Vidal, G. Saldarini

2002 **EUR 20520 EN**

EUROPEAN COMMISSION
JOINT RESEARCH CENTRE

Institute for the Protection and the Security of the Citizen
European Laboratory for Structural Assessment (ELSA)
I-21020 Ispra (VA) Italy

SEISLINES

Experimental Investigation of the Behaviour of Undeteriorated and Deteriorated Asbestos Cement Pipes under Seismic Loads (Task 5)

Final Report

P. Negro, D. Tirelli, J. Molina, G. Magonette, V. Vidal, G. Saldarini

2002 **EUR 20520 EN**

LEGAL NOTICE

A great deal of additional information on the
European Union is available on the Internet.
It can be accessed through the Europa server
(http://europa.eu.int)

EUR 20520 EN

Printed in Italy

SUMMARY

In this report the results of the experimental activities conducted in the European Laboratory for Structural Assessment of the Joint Research Centre as a part of the project Age-Variant Seismic Structural Reliability of Existing Underground Water Pipelines (SEISLINES) are described.

In particular, the report provides the results of the task 5 of such project, "Experimental Investigation of the Behaviour of Undeteriorated and Deteriorated Asbestos Cement Pipes Under Sesimic Loads".

The tests were conducted on straight segments of asbestos cement pipes, embedded in a volume of dry sand of well-known mechanical properties. Each segment had two 3 m long pipe elements connected by a standard steel joint. Two segments were tested at the same time, one in virgin (undeteriorated) conditions, the other having been chemically treated to reproduce the effects of the exposure to sulphate.

A description of the test setup is provided. Details on the artificial chemical deterioration procedure are given. The properties of the sand used in the experiments are reported. Finally, the results of the test are described, with a preliminary interpretation.

INTRODUCTION

The objective of the experimental activity was twofold.

From one side, the activity was aimed at deriving experimental data on the seismic behaviour of a realistic portion of an aqueduct line embedded in the soil in laboratory conditions. These data were needed for the assessment of the numerical models adopted in the study, so that calibration guidelines could be obtained and possible limitations of the models identified.

The other aspect was the effect of the chemical corrosion on the pipe segments, both for the material and the global behavior of the pipe-soil assemblage. It was decided to adopt asbestos cement pipes with an external diameter of 143 mm, 9 mm thick. The first phase was the commissioning and implementation of the artificial corrosion technique.

DEFINITION OF THE EXPERIMENTAL SETUP

The aim of the seismic tests was to obtain experimental information to be used in the assessment of the numerical models adopted for modelling the aqueduct lines, to highlight their eventual limitations, and to verify whether effects of corrosion on the global seismic behaviour exist.

The experimental set-up was defined (Figure 1) as a volume of dry sand of uniform and well-known mechanical properties, in which two pairs of pipe segments (one undeteriorated and one artificially corroded) were embedded. A steel caisson with dimensions 6.8 m x 2.2 m x 1.6 m (dept) was used (Figure 2). The sand used in an experimental activity previously carried out at ELSA was used, and the deposition technique was aimed at obtaining a uniform relative density.

The loading system was based on steel plates, controlled by hydraulic actuators underneath, to impose increasing upward distortion to the sand below the pipe, in correspondence to the joint.

Measurement had to include the imposed distortion and the corresponding measured force, as well as the rotation distribution along the length of the pipes.

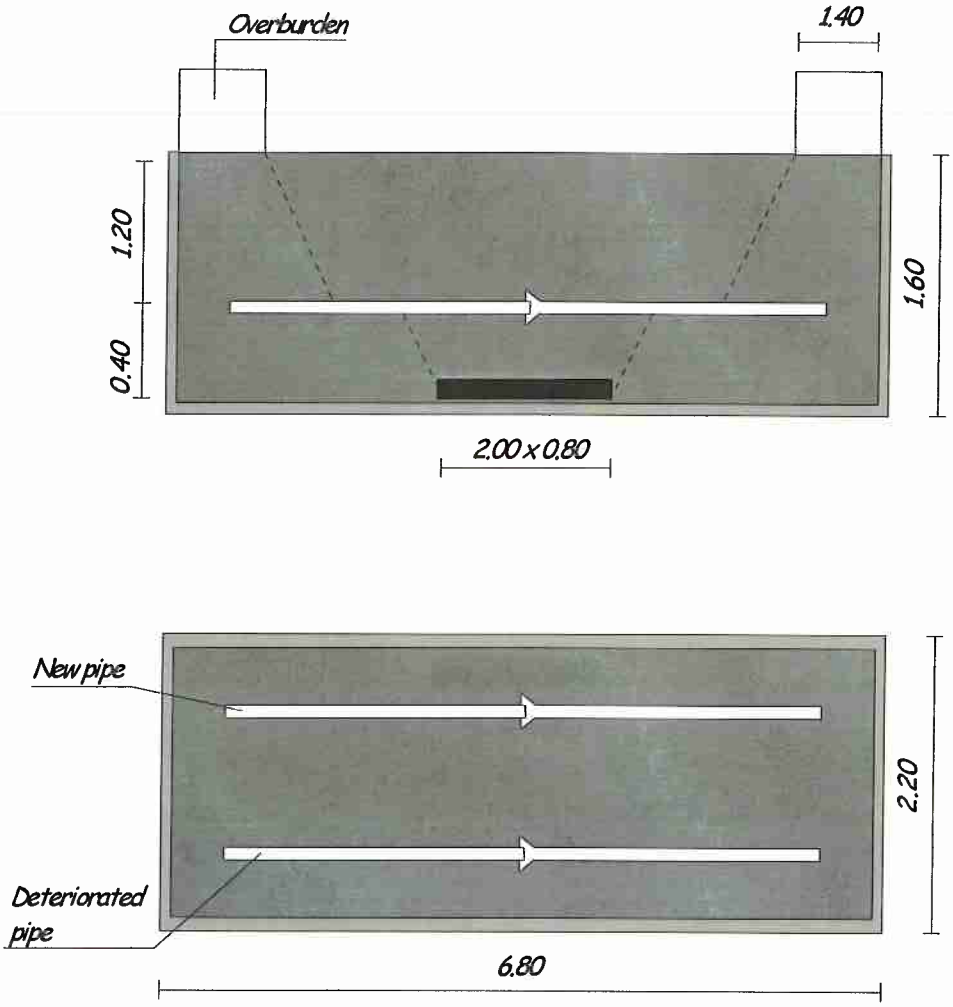

Fig. 1: Scheme of the experimental set-up for the seismic tests.

Fig. 2: Scheme of the experimental set-up for the seismic tests.

THE ARTIFICIAL CORROSION TECHNIQUE

For the artificial aging of the asbestos cement pipes, the aim was to expose the pipe segments to a severe, yet representative, sulphate attack. In order to accelerate the sulphate attack, the specimens were submerged in a 2.5% Na_2SO_4 solution. The concentration was intentionally set as much more aggressive than in any realistic soil condition, to accelerate the attack. To further accelerate the attack, the specimens were exposed to automatic wetting-drying daily cycles: when dried the specimens could be enriched in the sulphate content.

A special apparatus had to be designed and constructed to implement the technique, and this had to comply with necessary requirements as for the handling of the health hazardous materials, in particular asbestos powder.

The apparatus consisted of the following parts:

1. a specimen tank consisting in a prismatic plastic container, 3.2 m long, 1 m wide and 0.5 m high, provided with a removable airtight cover;
2. a secondary tank with 1500 litres capacity for storing the solution during the dry cycles;

Fig. 3: View of the apparatus for the artificial corrosion.

3. electric pumps to fill and empty the specimen tank;
4. pH regulating apparatus, to automatically correct the pH in the range 7 +/- 0.1;
5. a warm air generator, with the necessary filters;
6. a programmable control system.

The apparatus is shown in the Figure 3.

Two complete pipe segments were put in the tank, to be used in the seismic tests. In addition, 200 mm slices were also inserted and extracted after 1-2-3 months to perform the necessary mechanical and chemical qualification tests. These consisted of:

1. compressive strength tests, according to the European Norm EN 588-1;
2. measurement of the thickness of the samples;
3. water absorption;
4. XRD analysis to detect the secondary ettringite formation as opposed to the ettringite present in the undeteriorated pipe.

The value of the compressive strength did not indicate any significant damage, nor did the thickness measurements. The water absorption tests did not highlight any change in the porosity of the material. Chemical tests confirmed those based on the physico-mechanical aspects, in the sense that no secondary ettringite formation was found. The mechanical properties of the material exposed to the very aggressive sulphate environment did not show any significant change, highlighting the exceptional effectiveness of the asbestos fibres in reducing the porosity by means of a micro-reinforcement effect.
More details about the artificial corrosion technique are given in Appendix A.

CONSTRUCTION OF THE MODEL

Based on the definition of the experimental setup, the construction of the model was carried out. Two holes were cut in the floor of the caisson, and the loading apparatus was placed, as it is shown in Figure 4. A pneumatic ring tube was placed between the caisson floor and the steel loading plate, to prevent the sand from flowing underneath the plate when it moved upwards.

The first layer of sand was placed. Sand of well known mechanical properties was adopted. A comprehensive description of both chemical and mechanical properties of the sand is provided in Appendix B. The sand was placed by letting it fall from a narrow orifice from a constant height (Figure 5). This procedure was adopted in other experimental activities (Faccioli et al., 1999; Negro et al., 2000), and is known to result into uniform relative density (Jamiolkowski, 1999). No particular value of the target density was selected, instead, four moulds of known volume were placed. The resulting relative density was found to be substantially uniform, with a mean value of 38%.

Fig. 4: View of the loading apparatus.

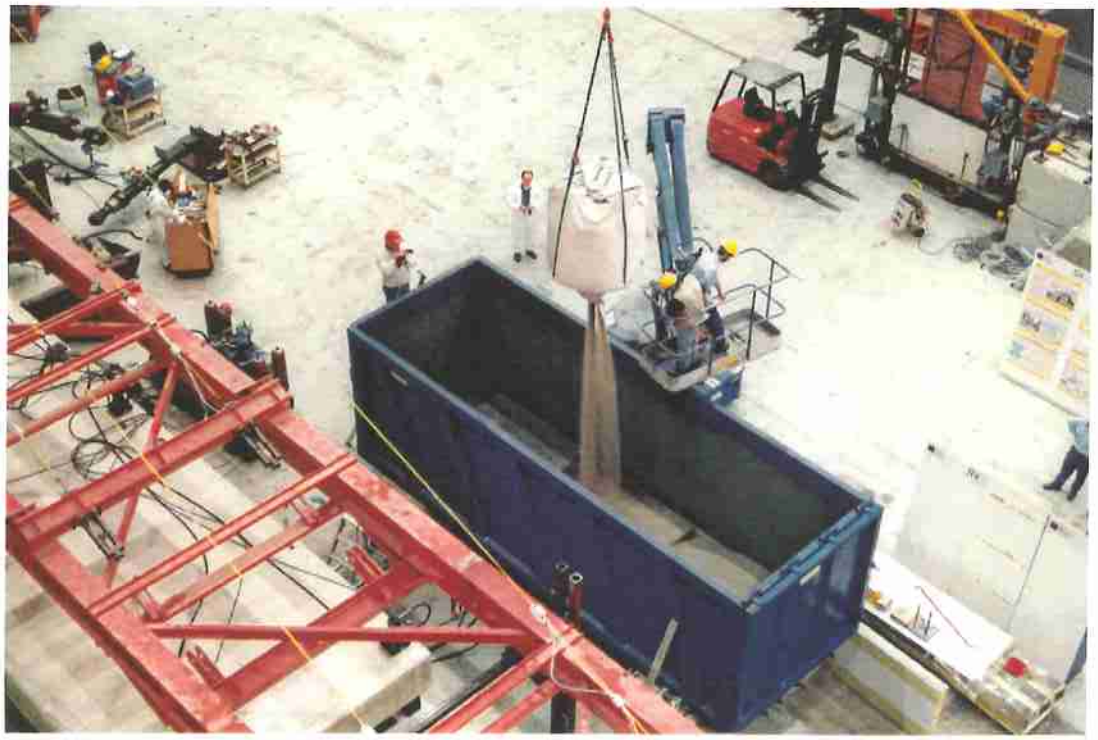

Fig. 5: Deposition of the sand.

After the first layer of sand had been positioned, the pipe segments were placed. The steel joints were mounted, and sealing blocks were placed at the ends of the segments. The tubes for filling the pipes with water were connected and the steel rods for measuring the vertical displacement were placed. A water pressure of 1.5 m was applied. A number of micro-inclinometers were glued to the surfaces of the pipes.

The upper layer of sand was placed, by using the same technique The thickness of the layer was finally set as 0.9 m. The reaction blocks were positioned, and connected to the strong-floor of the laboratory.

The construction of the specimen is illustrated by the following figures, and the final setup and instrumentation layout is depicted in the schemes.

Fig. 6: Placement of the steel joint.

Fig. 7: General views of the experimental setup.

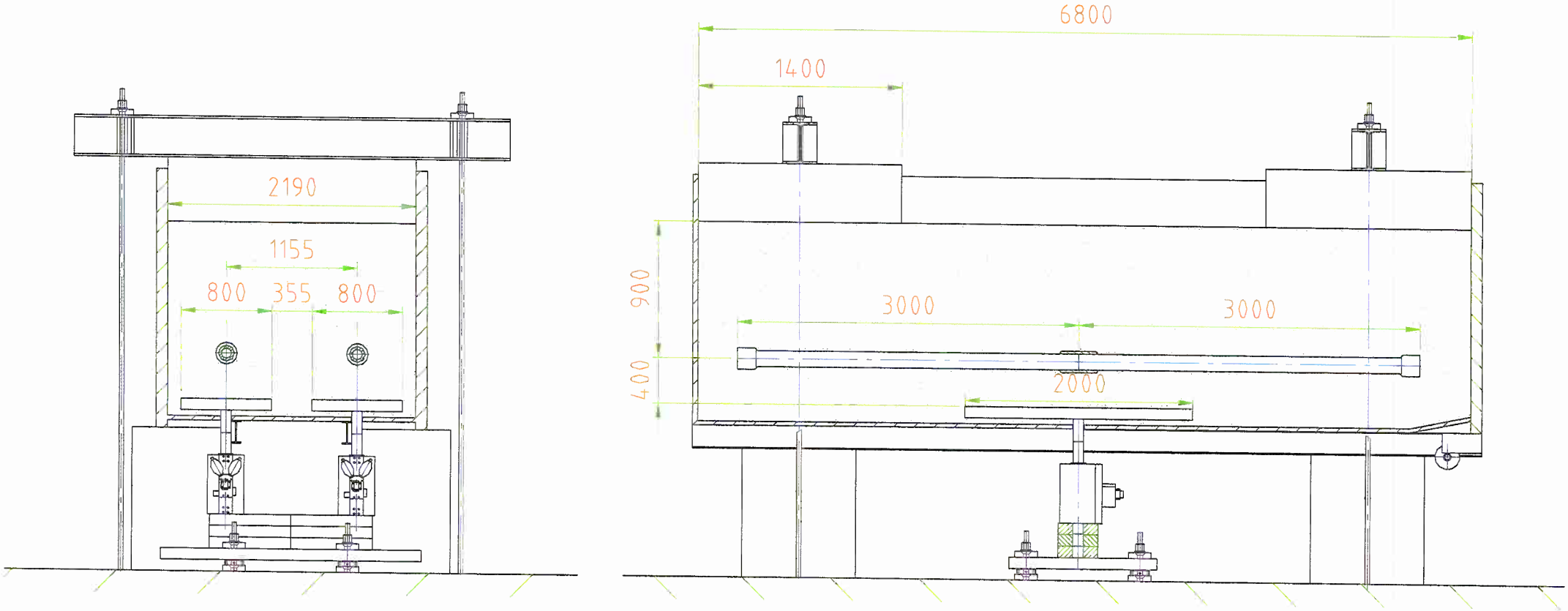

Fig. 8: Scheme of the experimental setup.

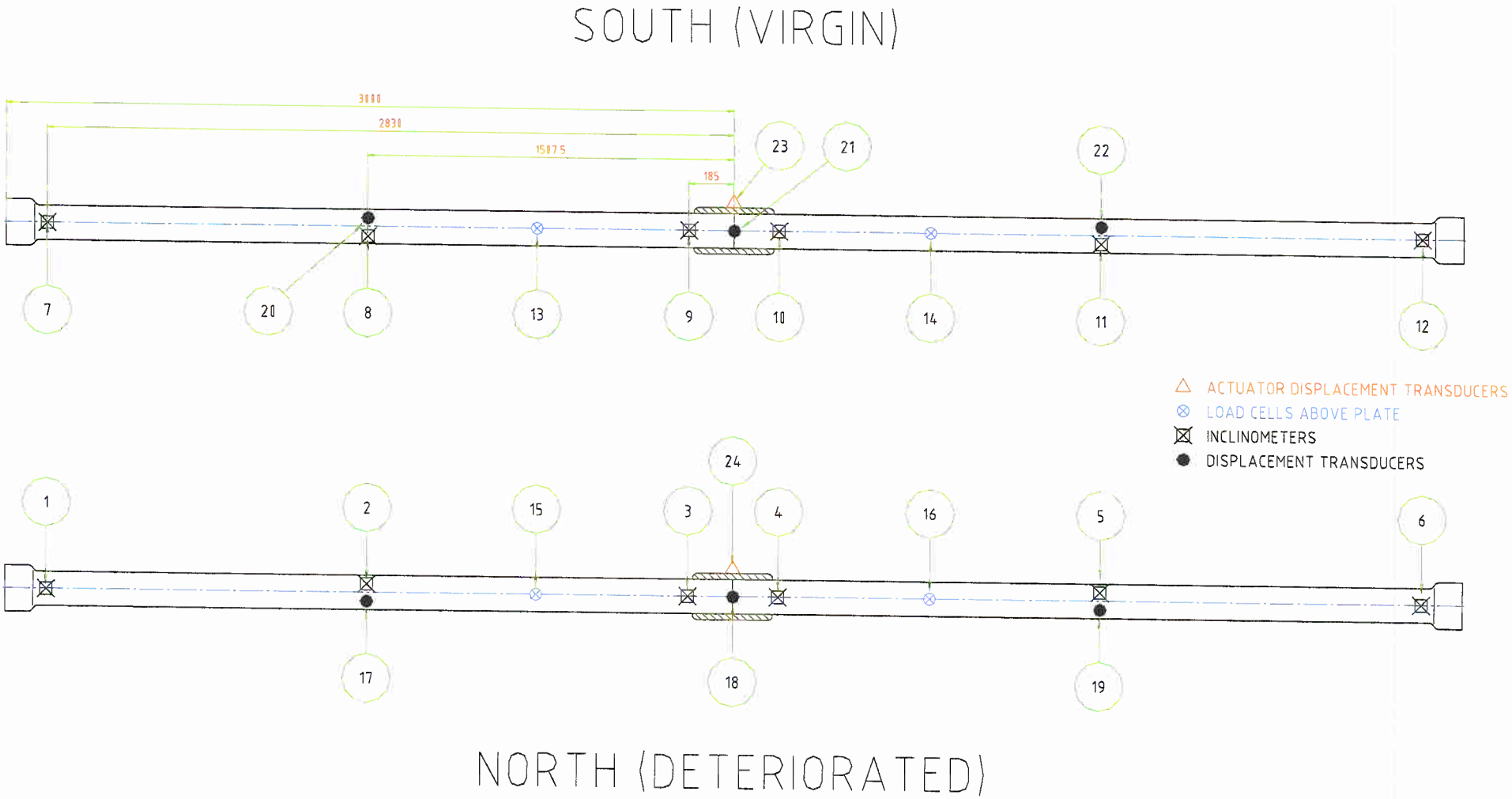

Fig. 9: Scheme of the instrumentation.

TEST SEQUENCE

The test sequence consisted of a single monotonic displacement ramp to be imposed to the steel plates. It was decided to test the two segments (virgin and deteriorated) in tandem, i.e., in a unique test. This decision was made to avoid possible disturbances of the sand surrounding the specimen not being tested.

Unfortunately, during the first part of the test one of the actuators did not react to the command signal, therefore the test had to be stopped and that actuator had to be positioned manually to reach the same displacement reached by the other. During this manual phase the acquisition of the measurement was not possible. As a result, the first phase of the loading was not recorded for this actuator, and some distortion of the sand interface could have taken place. Even though the first loading sequence was not recorded, the initial values were, therefore the results of the rest of the test could be referred to the initial conditions. The test was continued far beyond the failure of the segments (which was highlighted by a sudden drop of the reaction force, as well as a drop in the water pressure), up to the complete loss of residual stiffness.

TEST RESULTS – PRELIMINARY INTERPRETATION OF RESULTS

The results are presented in the following figures. The possibly most important piece of results is the comparison of the global force-displacement diagram for the two segments (Figure 10). The graph starts at a value of the load of 60 kN for the reasons explained in the previous paragraph. The corroded segment, represented by the red curve, breaks at a displacement of about 15 mm, much smaller than the displacement at which the virgin segment, represented by the blue curve, does (about 32 mm). However, these displacements could have been affected by the disturbance introduced by the first loading phase, which was asynchronous. This statement is supported by the fact that the loads at which the two segments broke are rather similar (81 kN for the corroded segment, 84 kN for the virgin segment). From this graph, no major differences in the behaviour of the two segments could be inferred, thus confirming the findings of the artificial corrosion.

In Figure 11 the vertical displacements measured at different positions along the segments are given as a function of the imposed displacement. The graph on the right hand side refers to the virgin (undeteriorated) segment, the other to the corroded one. One should refer to Figure 9 to identify each curve: the number in the scheme corresponds to the last two digits in the label. The behaviours of the two segments are similar, and most of the vertical deformation took place at the joint, thus demonstrating that the ends of the segments were adequately restrained, a condition which was requested for the test setup to be representative of the seismic behaviour of a real aqueduct line. The vertical displacements of the segments at failure (about 20 mm for the virgin segment and 15 mm for the corroded one) are much closer apart than the corresponding displacements imposed at the level of the loading plate. This is further evidence that the behaviours of the virgin and corroded segments were similar.

In Figure 12 the measurement of the inclinometers are depicted as a function of the imposed displacement. The graph on the right hand side refers to the virgin (undeteriorated) segment, the other to the corroded one. Again, one should refer to Figure 9 to identify the position of each sensor. No major differences between the behaviour of the virgin and deteriorated segments are visible. The point corresponding to the first rupture is clearly identifiable in the graphs, and by identifying the curves in which the drop takes place, one can conclude that the rupture took place in the vicinity of the joint.

CONCLUSIONS

The testing activity conducted on portions of asbestos cement water pipelines was presented. This included the experimental assessment of the differences in the seismic behaviour which could be due to the exposure of the pipes to chemically aggressive environment.
It was proved that the effects of chemical attacks from sulphate are negligible, for the material of the pipes as well as for the global seismic behaviour of the pipeline.
The results of the test were used to verify the models used in the project and could represent a wealth of information against which more refined model could be calibrated or developed.

REFERENCES

FACCIOLI E, PAOLUCCI R., VANINI M. (Eds.) - "3D Site Effects and Soil-Foundation Interaction in Earthquake and Vibration Risk Evaluation", European Commission, Brussels, 1999.

NEGRO P, PAOLUCCI R., PEDRETTI S., FACCIOLI E. - "Large Scale Soil-Structure Interaction Experiments on Sand Under Cyclic Loading", *12th World Conference on Earthquake Engineering*, Auckland, New Zealand, January 30 - February 4, 2000.

JAMIOLKOWSKI M., LO PRESTI D.C.F., PUCI I., NEGRO P., VERZELETTI G., MOLINA J.F., FACCIOLI E., PEDRETTI S., PEDRONI S., MORABITO P. - "Large Scale Geotechnical Experiments on Soil-Foundation Interaction", *2nd International Symposium on Pre-Failure Characteristics of Geomaterials*, Turin, 27-29 September 1999.

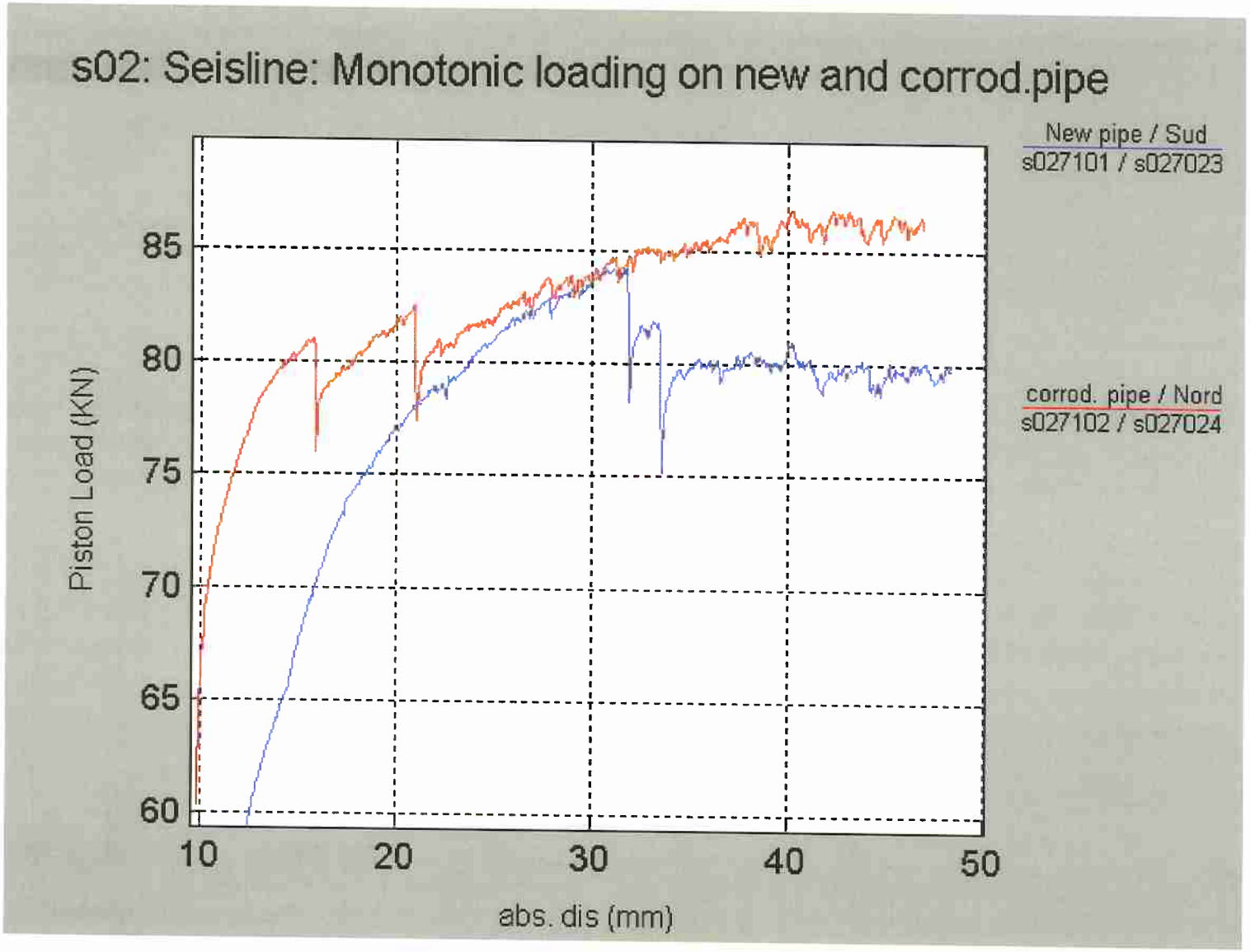

Fig. 10: Measured monotonic force-displacement diagrams.

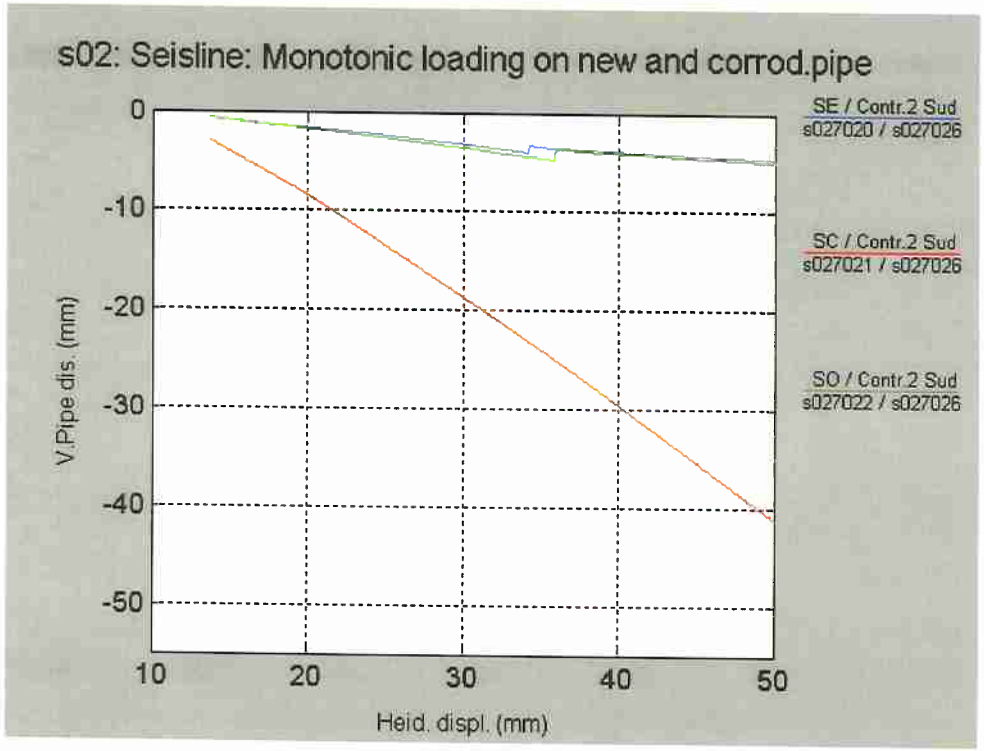

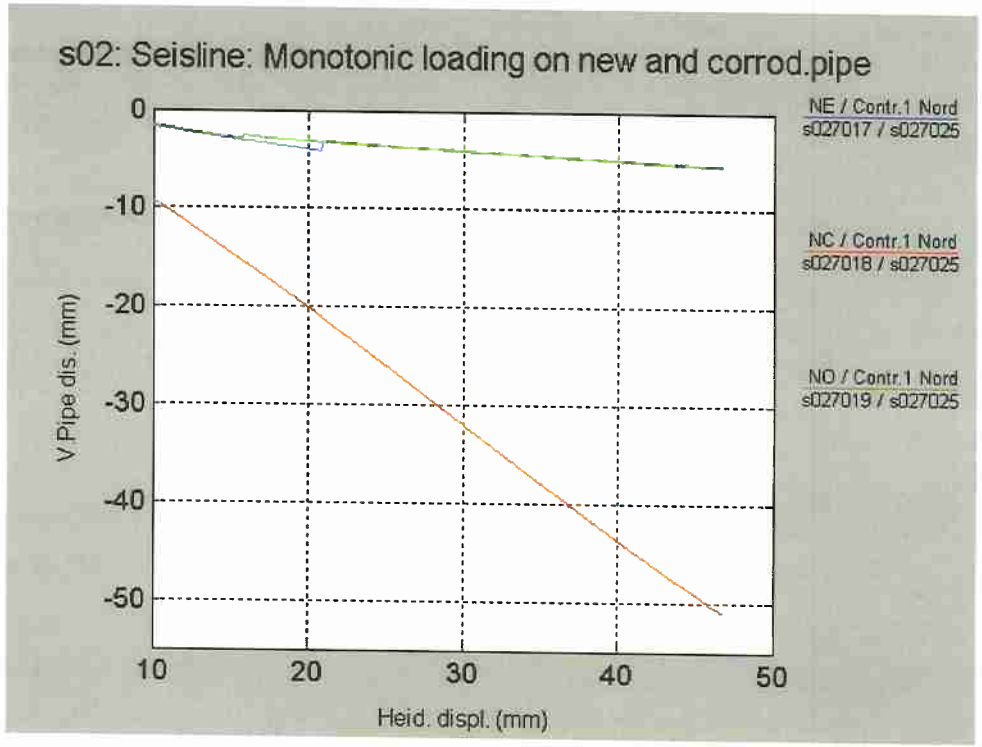

Fig. 11: Measured distributions of vertical deformation along the pipes.

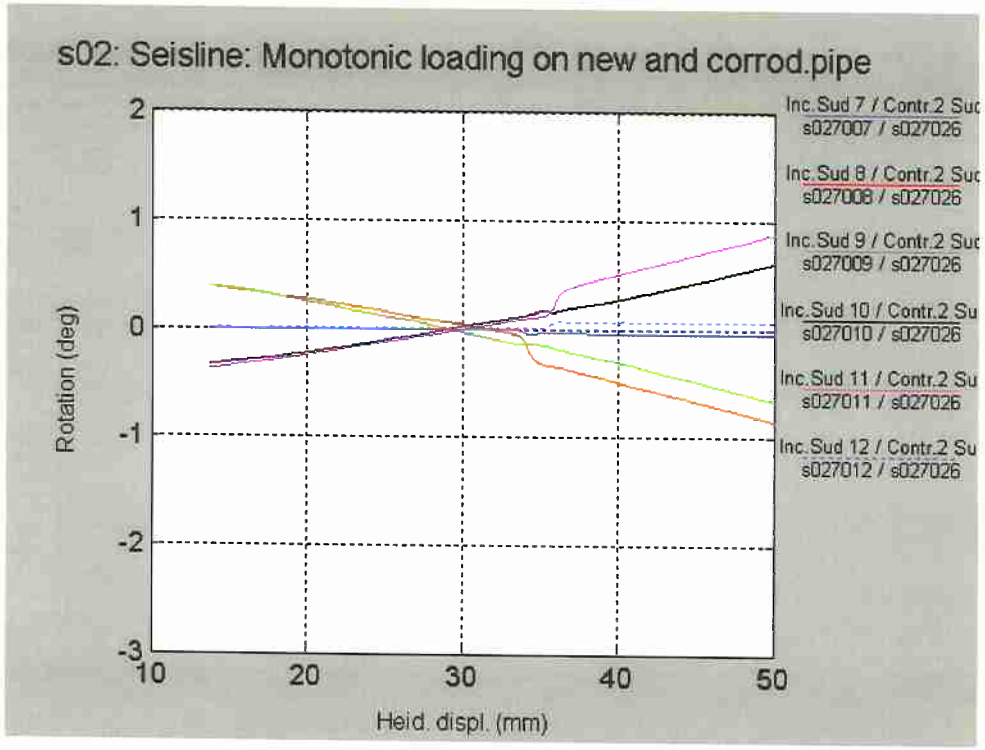

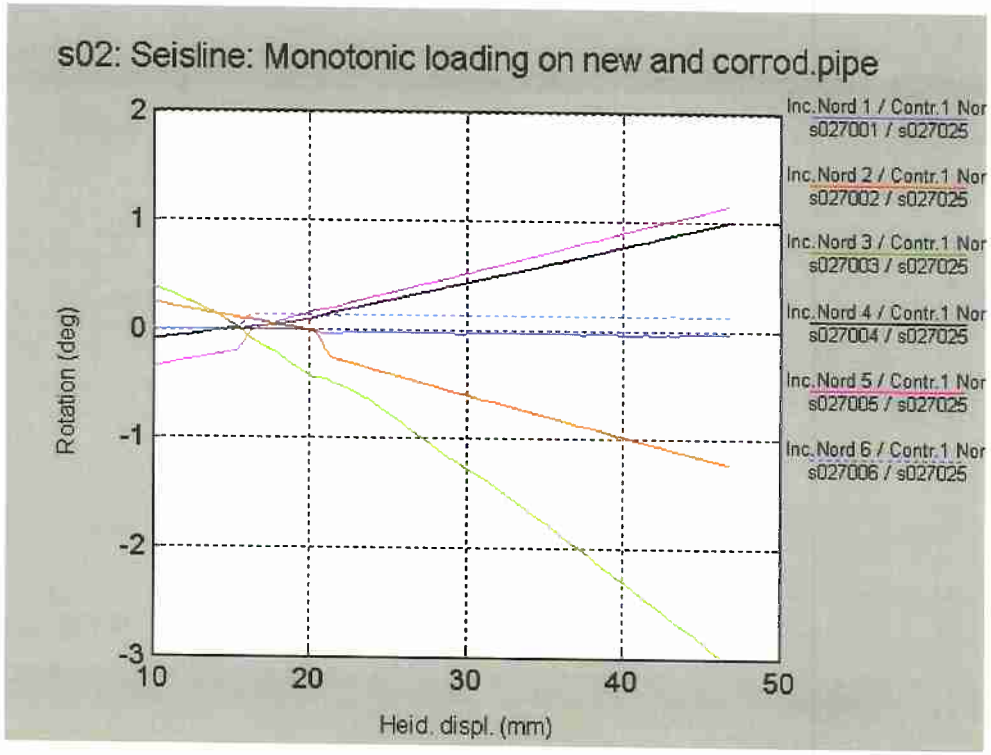

Fig. 12: Measured distributions of rotation along the pipes.

APPENDIX A: DESCRIPTION OF THE ARTIFICIAL CORROSION TECHNIQUE

ARTIFICIAL AGING OF ASBESTOS-CEMENT PIPES

Prof. Mario Collepardi
Ing. Silvia Collepardi
Ing. Roberto Troli

1. INTRODUCTION

Cement-based pipes embedded in soil can be deteriorated by the leaching effect of the water transported inside the pipes and/or by the chemical attack due to the presence of some salts in the soil.

According to the European Norm EN 206 the main ingredient in the soil which can attack cement-based materials is the sulphate.

2. INTERACTION OF SULPHATE-CEMENT

There are two types of interaction between sulphate and cement, both related to the formation of a chemical product called ettringite ($C_3A \cdot 3CaSO_4 \cdot 32H_2O$):

- Early Ettringite Formation (*EEF*) producing "primary" ettringite
- Delayed Ettringite Formation (*DEF*) producing "secondary" ettringite

2.1 Early Ettringite Formation

Sulphate, in form of gypsum ($CaSO_4 \cdot 2H_2O$) is already present in the cement (about 5%) in order to regulate the setting of cement. In the absence of gypsum there is quick set due to a very rapid reaction of calcium alluminate (C_3A) and water producing hexagonal crystals of hydrated calcium alluminate C-A-H (Fig. 1, above).

In the presence of gypsum, water and C_3A react to **produce "primary"ettringite immediately** (*EEF*) in form of a coating around the C_3A grains (Fig. 1, below). Due to the ettringite coating the rate of C_3A hydration (V_2) is much lower than that (V_1) which occurs in the absence of gypsum. For this reason gypsum plays an important role in the cement hydration as set regulator through the early ettringite formation according to this chemical reaction.

$$\underset{\text{(calcium aluminate)}}{C_3A} + \underset{\text{(gypsum)}}{3CaSO_4 \cdot 2H_2O} + \underset{\text{(water)}}{26H_2O} \Rightarrow \underset{\text{(ettringite)}}{C_3A \cdot 3CaSO_4 \cdot 32H_2O} \quad [1]$$

The reaction [1] producing ettringite is accompanied by a volume increase since the specific weight of ettringite is much lower than that of the reactants (C_3A, gypsum and water). The volume increase due to the early ettringite formation occurs when the water-cement system (in form of a paste, mortar or concrete) is still plastic, that is with a very low elastic modulus.

Therefore the expansion related to the ettringite formation does not produce any disruptive effect since the cement matrix can be easily deformed. An other important aspect of the *EEF* is the uniform distribution of ettringite throughout the system.

Than *EEF* is useful for the set regulation without any harmful effect since is occurs **immediately** and **homogeneously**.

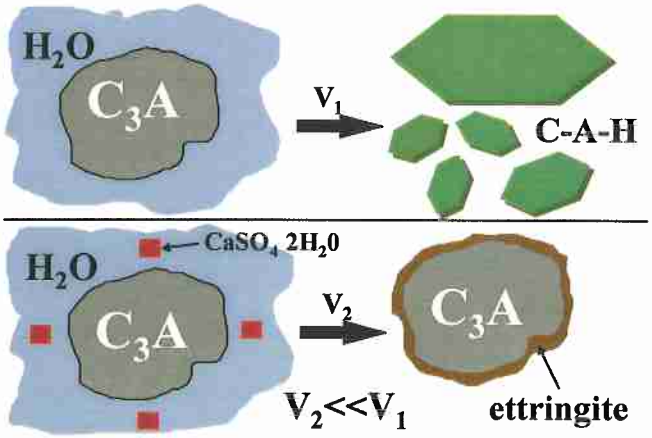

Fig. 1 – The hydration of C_3A in the absence (above) and in presence of gypsum (below).

2.2 Delayed Ettringite Formation

Delayed ettringite formation (*DEF*) is associated with a damaging effect because it occurs **later** and **heterogeneously**.

Figure 2 shows schematically the main differences between *EEF* and *DEF*, as well as the two type of *DEF : ESA* (External Sulphate Attack) and *ISA* (Internal Sulphate Attack). The type of *DEF* for the cement-based structures embedded in a soil is related to the sulphate attack from the environment, that is the sulphate present in the soil. Therefore, this is considered to be an *ESA* type of *DEF* with formation of "secondary" ettringite which must be distinguished from "primary" ettringite formed earlier in the setting period of cement.

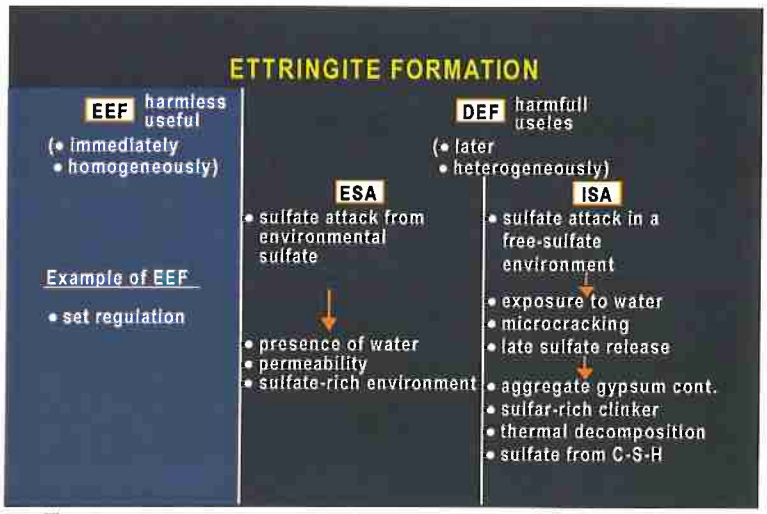

Fig. 2 – Schematic representation of EEF and DEF.

Figure 3 schematically shows the three factors needed for the Delayed Ettringite Formation (*DEF*) caused by External Sulphate Attack (*ESA*); they are the permeability of the cement based material, the presence of water and sulphate rich environment. In the absence of one of these factors the *ESA* cannot occur. For instance if the cement-based structure is crack-free and is made by a very dense material with low capillary porosity (low permeability) the sulphate ions cannot diffuse from the environment through the water filling the capillary pores or the cracks. On the other hand, a permeable cement-based structure cannot be penetrated by sulphate ions in a dry soil since, in the absence of water, sulphate ions cannot migrate through the cement matrix. Finally it is trivial that, in the absence of sulphate in the environment any sulphate attack cannot occur.

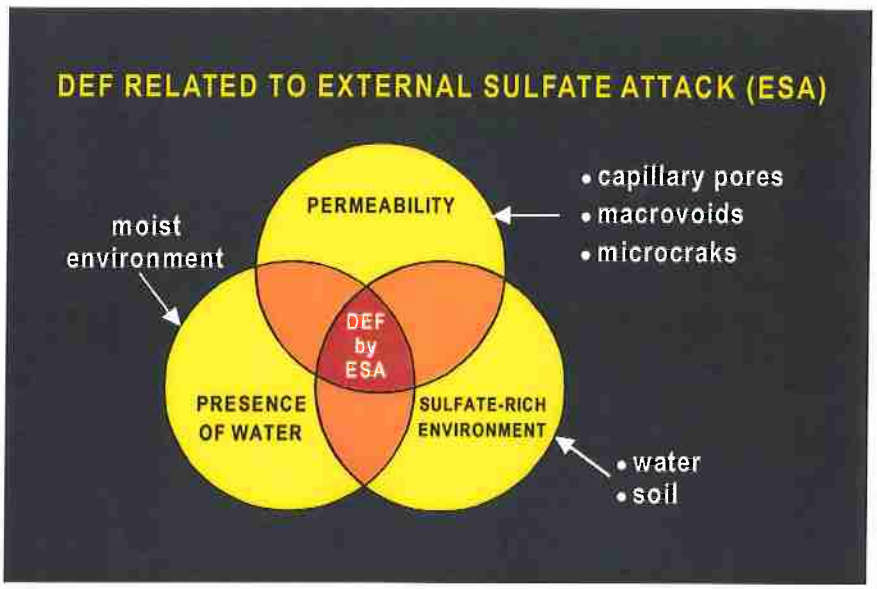

Fig. 3 – The coexistence of permeability, presence of water and sulphate rich environment is needed for the Delayed Ettringite Formation (DEF) caused by External Sulphate Attack (ESA).

The reason why *DEF* related to *ESA* is very harmfull is due to the localized formation of ettringite. For instance, in a concrete canal transporting sulphate-rich water ettringite is formed only on the skin of the concrete in contact with the water. The ettringite formation occurs with an expansive character (volume increase) and this is responsible for a disruptive action because the expansion occurs only on the skin and does not involve uniformly the interior part of the structure. On the other hand, this localized exspansion occurs in a rigid system and then the expansion is transformed into a tensile stress for the skin which is delaminated.

Therefore *ESA* is very harmfull due to the localized formation of "secondary" ettringite. For instance, in a concrete canal transporting sulphate-rich water ettringite is formed only on the skin of the concrete in contact with the water (Fig. 4). On the other hand, this localized expansion occurs in a rigid system and then the expansion is transformed into a tensile stress for the skin which is delaminated.

Therefore *DEF* by *ESA* related to the formation of "secondary" ettringite is dangerous and responsible for deterioration of concrete structures, whereas the formation of "primary" ettringite related to the set regulation is not dangerous. This distinction between "primary" and "secondary" ettringite (related to *EEF* and *DEF* respectively) is very important for the interpretation of diagnostic data based on the detection of ettringite as those determined, for instance, by X-Ray Diffraction (*XRD*) analysis.

Fig. 4 – Typical external sulphate attack (ESA) occurring on the surface of the concrete of a canal in contact with a sulphate rich water. After removing water, deterioration by ESA can be observed.

3. PURPOSE OF THE RESEARCH

The purpose of the research is finalized to study the behaviour of asbestos-cement pipes embedded in sulphate rich-soil. The durability of this type of cement based materials is a very important problem due to the risk of asbestos fibers, liberated by the deteriorated cement system, for the health of human beings.

4. EXPERIMENTAL

Asbestos cement pipe specimens, about 200 mm long and with a diameter of about 140 mm, were obtained by cutting some real pipes 2 m or 3 m long.

In order to accelerate the sulphate attack the pipe specimens were submerged in a 2.5% Na_2SO_4 aqueous solution which is much more aggressive than a soil with the corresponding sulphate content, because, sulphate ions can penetrate the cement matrix of the pipes much more quickly through an aqueous environment than through a solid environment such as a soil.

Moreover, in order to accelerate additionally the sulphate attack the pipe specimens were exposed to automatically wetting-drying daily cycles: when dried the specimens could be enriched in the sulphate content.

After some months of exposure to the sulphate aqueous solution the following properties were determined to check the deterioration by sulphate attack, if any:

a) compressive strength;
b) change in the thickness of the pipe;
c) water absorption;
d) XRD analysis to detect the "secondary" ettringite formation with respect to the "primary" ettringite present in the pipe specimens not exposed to the sulphate attack.

All the results will be examined in the following paragraphs devoted to phisyco-mechanical and chemical tests.

4.1 Wetting-Drying equipment

In order to produce the wetting-drying cycles, a special automatic apparatus was set up. The apparatus consisted of the following parts:

1. a specimens tank consisting in a prismatic plastic container having 3200 mm long, 1000 mm wide and 500 mm high provided with a removable airtight cover. In this tank the asbestos cement pipes were laid on special supports and submitted to the wetting-drying cycles;
2. a secondary tank consisting in a cylindrical container having 1500 litres of capacity used as storing tank for the solution during the drying phase of the cycles;
3. two electric pumps (an emptying pump and an adduction pump) connected to the tanks with a proper set of pipes, flanges, joints and valves. The pumps had to transfer the solution into and out of the specimens tank during the wetting-drying cycles.
4. a pH regulating apparatus able to measure and automatically correct the pH of the solution in the range of 7 ± 1;
5. a warm air generator having the task of inflating warm air in the specimens tank in order to dry the specimens during the period in which the tank was empty of water;
6. a programmable controlling system able to manage automatic cycles of filling and emptying (and air drying) of the specimens tank.

4.2 Physico-mechanical tests

The phsyco-mechanical test including the measurements of the compressive strength, the pipe thickness and the water absorption are shown in Table 1 for the pipe specimens not exposed to the sulphate solution or exposed for 1-2-3 months.

The compressive strength was determined by the following equation [2] according to the European Norm EN 588-1:

$$R = n \cdot F\left(\frac{3d_i + 5l}{L \cdot e^2}\right) \qquad [2]$$

where R is the compressive strength, d_i is the internal diameter, e is the thickness of the pipe, L is the length of the pipe, F is the load applied to break the pipe, C is the load/length (F/L) ratio, and n is a factor assumed to be 0.3 for pipes with diameter different from 100 mm.

The values of compressive strength (R) determined by equation [2] and shown in Table 1 indicate that there is not any significant damage related to a strength reduction. Indead, all the compressive strength of the pipes exposed to the very aggressive sulphate environment are into the range of 19-26 MPa of the pipes not exposed to sulphate.

Even the thickness does not result to be reduced for the sulphate attack (Table 1). All the thickness values of the pipe specimens exposed to the sulphate aggression are into the range of 8.5-9.6 mm of the pipes not exposed to sulphate.

Table 1 – mechanical (strength) and physical (absorption) properties of asbestos-cement types.

Time of exposure to sulphate (months)	Weight (g)	Length (mm)	External Diameter (mm)	Thickness (mm)	Inside Diameter (mm)	Load (kgf)	Load/Length ratio (kN/m)	Compressive strength (N/mm^2)	Water absorption (%)
0	1313.9	193.0	141.12	9.6	121.92	280	14.2	**19.1**	**6.71**
	1440.1	196.2	141.89	8.5	121.92	310	15.5	**26.2**	\
1	1461.7	196.4	141.12	9.1	121.92	320	16.0	**23.8**	**5.89**
	1363.6	196.7	141.12	9.8	121.92	310	15.4	**20.0**	**5.79**
2	1405.2	197.7	140.4	8.6	121.92	240	11.9	**19.7**	\
	1467.3	197.3	141.5	8.1	121.92	240	11.9	**22.1**	**7.65**
3	1512.0	201.6	141.8	9.27	121.92	340	16.5	**23.8**	**5.93**
	1455.3	199.1	141.2	8.54	121.92	300	14.8	**24.8**	\

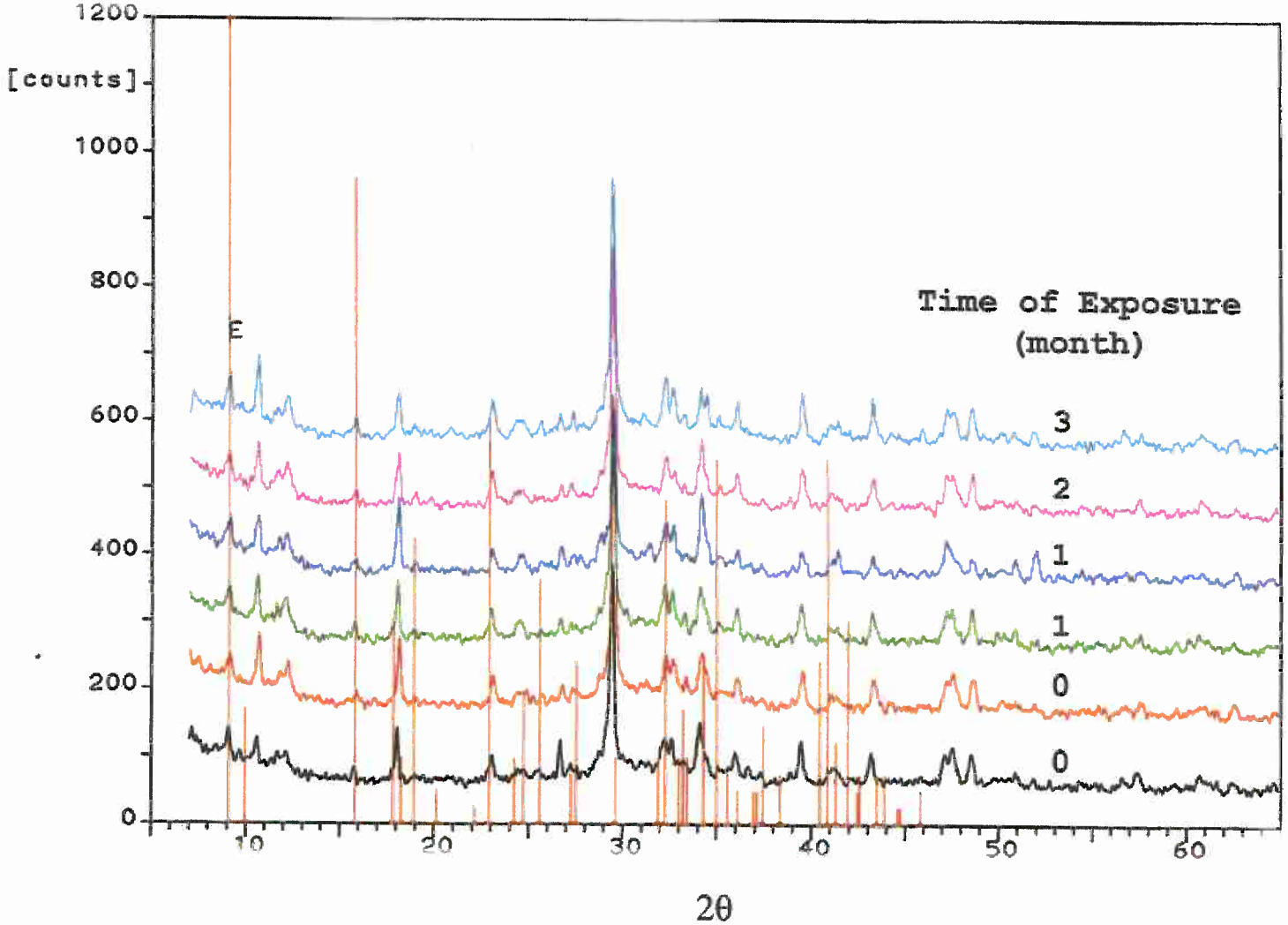

Fig. 5 – XRD patterns of specimens exposed to sulphate for different times.

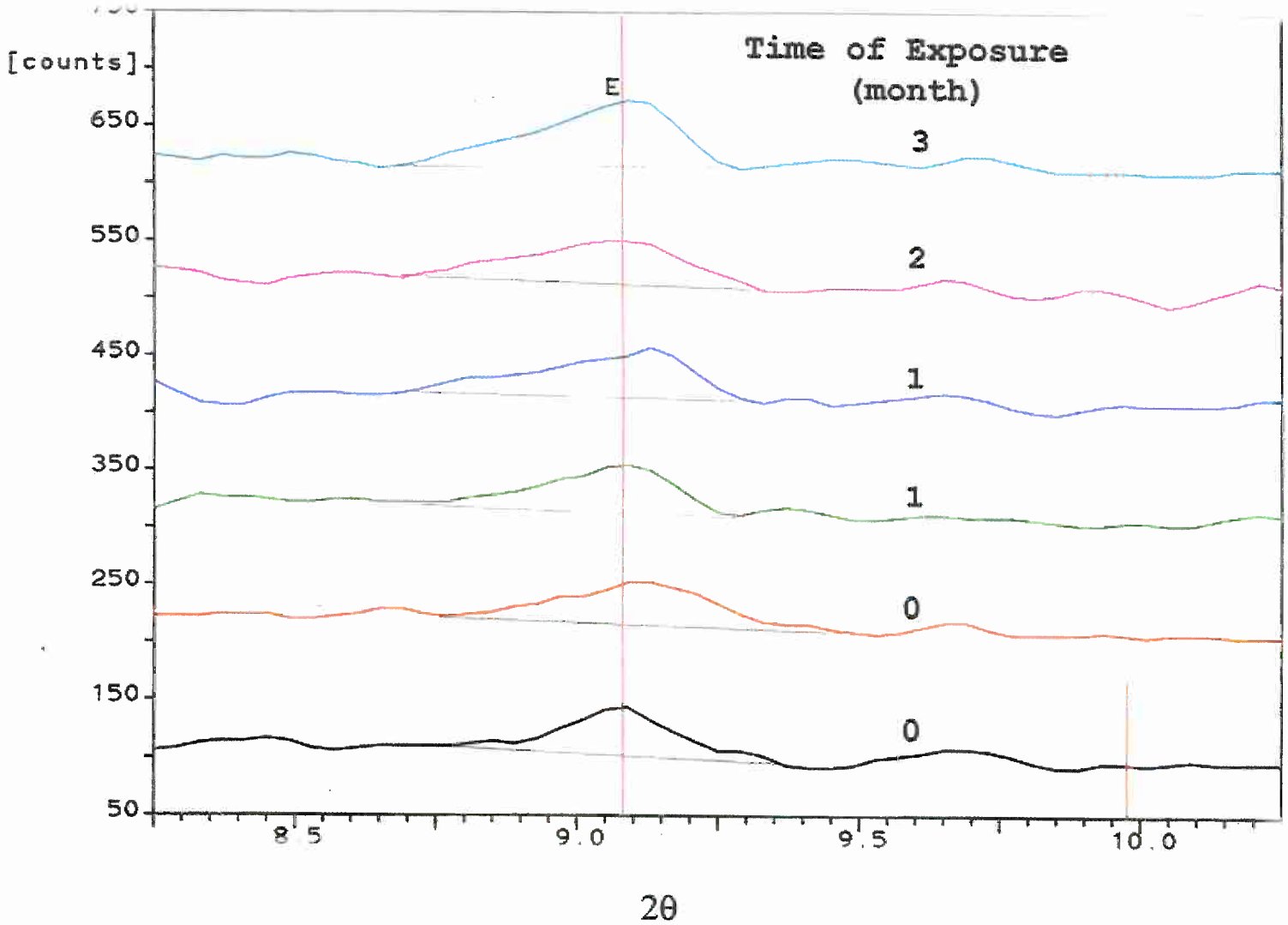

Fig. 6 – Details of XRD main peak of ettringite at 9.08 as a function of the time exposure to sulphate environment.

The measurement of water absorption was carried out by drying at 110°C a piece of the pipe specimens and then saturating by water the material. The percentage change in the weight of the water saturated specimen with respect to the dried one, is the water absorption. Again the absorption values, related to the capillary porosity of the cement matrix does not change for the exposure to the sulphate environment. Moreover, the values of 5-6% of water absorption indicate that the quality of the cement matrix, where the asbestos fibres are embedded, is very good in terms of low porosity and then of water penetration.

4.2 Chemical tests

The specimens of pipes were finally ground and subjected to X-Ray Diffraction (*XRD*) analysis.

Figure 5 shows the XRD patterns of the specimens as a function of the time of exposure to sulphate. For each *XRD* pattern there are many peaks. For instance the *XRD* peaks of ettringite are evidenced by the vertical lines overlapping them.

The amount of ettringite is proportional to the area under the main peak at 9,08°. There is no significant difference between the peak of the "primary" ettringite (*EEF*) detected on the virgin specimens not exposed to sulphate and those of the pipe specimens exposed to sulphate. This means that no "secondary" ettringite if formed by *DEF* related to *ESA*.

Figure 6 shows the enlarged ettringite peak at 9.08°. The area under the peak in proportional to the amount of ettringite. Again no significant change is observed in the area under the peak at 9.08° by increasing the exposure time to sulphate.

Therefore chemical tests based on the *XRD* data confirm those based on the phsyco-mechanical tests and indicate that, due to the good quality of the cement matrix in terms of low porosity and absence of microcracks, the *DEF* by *ESA* cannot occur for the absence of one the three factors (*permeability*) needed for this type of deterioration.

5. CONCLUSIONS

The quality of the cement-based material is very good. In particular, the capillary porosity is very low and the cracks are absent due to the presence of the very effective reinforcement of the asbestos fibers.

Since sulphate cannot penetrate the cement matrix there is no deterioration at all although the pipe specimens were exposed to a very aggressive exposure for the sulphate concentration (25.000 mg/L of Na_2SO_4 aqueous solution) aggravated by wetting-drying daily cycles.

There is a good agreement between the physico-mechanical test and the chemical ones. No decrease in the compressive strength and in the thickness of the pipe were recorded. These results agree very well with no appearance of harmfull "secondary" ettringite in addition to the harmless "primary" ettringite formed initially before the exsposure to the aggressive sulphate aqueous solution in the virgin pipes.

Enco Srl
Prof. Mario Collepardi
Ing. Silvia Collepardi
Ing. Roberto Troli

APPENDIX B: PHYSICAL AND MECHANICAL PROPERTIES OF THE TEST SOIL MATERIAL (TICINO SAND)

PHYSICAL AND MECHANICAL PROPERTIES OF THE TEST SOIL MATERIAL (TICINO SAND)

Ticino sand (TIS), from the Ponte della Becca site (Pavia, Italy), processed for elimination of fines prior to testing, was used for the test. It is uniform, coarse-to-medium silica sand, with sub-angular grains having sphericity from 0.7 to 0.8. The grain size distribution is given in Fig. B.1. The crushability of this sand is evaluated by means of various indexes (Bellotti et al. 1991). It was found that a measurable crushability had occurred for this sand as well as for other silica or quartz sands only in the case where normal stresses exceeded 10 to 25 MPa (Bellotti et al. 1991, Fioravante et al. 1997).

In Table B.1 the maximum and minimum dry soil unit weight (γ_{dmax}, γ_{dmin}), the grain specific weight G_s, the mean diameter D_{50} and the uniformity coefficient Cu are given. In Table B.2 mineralogical composition of the sand is specified. Fig. B.2 shows a magnified image of Ticino sand particles.

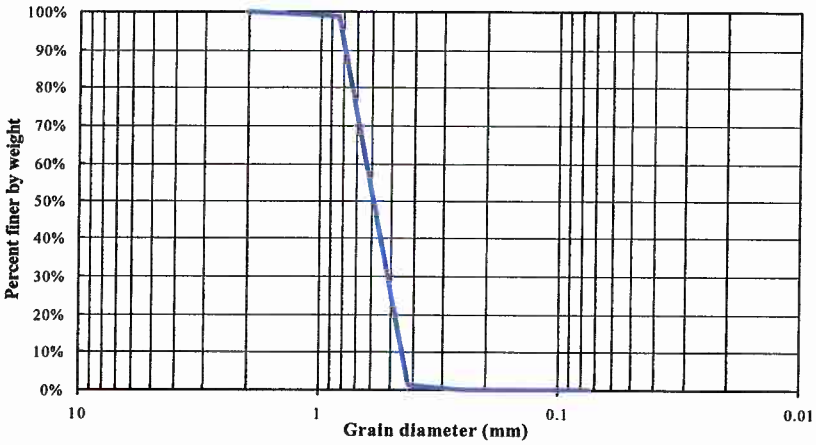

Fig. B.1: Grain size distribution of Ticino sand

Table B.1: Physical properties of Ticino sand

γ_{dmax}	γ_{dmin}	G_s	D_{50}	Cu	e_{min}	e_{max}
1.689 g/cm^3	1.391 g/cm^3	2.684	0.55 mm	1.6	0.579	0.931

Table B.2: Mineralogical and morphological characteristics of Ticino Sand

Mineral	**(%)**	**Angularity**	(%)	**Sphericity**	(%)
Quartz	33	*Very angular*	-	***0.4-0.5***	3.2
Feldspars	26	***Angular***	19.0	***0.5-0.6***	6.5
Rock fragments	37	***Subangular***	54.6	***0.6-0.7***	19.8
Other minerals	4	***Subrounded***	26	***0.7-0.8***	44.0
		Rounded	-	***0.8-0.9***	16.3
		Very rounded	-	***0.9-1.0***	10.3

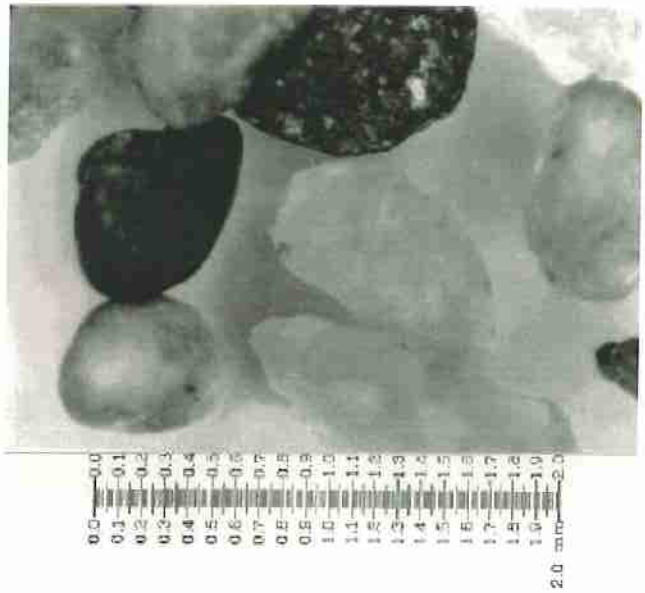

Fig. B.2: Ticino sand particles grains magnified by a factor of 40 (Rondena 1984)

Strength parameters

The peak shear resistance angle ϕ'_p of Ticino sand is given by:

$$\phi'_p = \phi'_{cv} + 0.0346\, D_R \left[10 - \ln(p'_f)\right] - 3.46 \qquad (B.1)$$

where ϕ'_{cv} is the shear resistance angle at constant volume, equal to 34.6°, p'_f the mean effective pressure (in kPa) and D_R the relative density (in %). The cohesion c' is zero. The above relationship (Bolton, 1986) is obtained from drained compression loading triaxial test, by means of regression analysis of a large database (≅ 400 tests).

According to eq. (B.1) φ_p increases with relative density and decreases with the mean stress at failure. This equation enables one to account for stress-dilatancy in an empirical and a simplified way.

Sand deformability at small strain

Ticino sand exhibits an anisotropic elastic behaviour (Bellotti et al. 1996) that can, however, become significant only for large horizontal stresses. The shear modulus in the vertical plane G_0 and the Young Modulus in the vertical direction E_0 are independent of each other in a transversely isotropic medium. For this reason in the small strain range ($\varepsilon < 10^{-5}$) different relationships are used to estimate the elastic moduli (Lo Presti et al. 1997):

$$G_0 = S_1 \frac{(2.27-e)^2}{1+e} p_a \left(\frac{s'}{p_a}\right)^{n1} \qquad E_0 = S_2 \frac{(2.17-e)^2}{1+e} p_a \left(\frac{\sigma'_v}{p_a}\right)^{n2} \quad (B.2)$$

where e is the void ratio, p_a the atmospheric pressure, $s=(\sigma'_v+\sigma'_h)/2$, σ'_v and σ'_h vertical and horizontal effective stresses, $S_1 = 710$, $S_2 = 1510$, $n_1 = 0.43$, $n_2 = 0.53$.

Non-linear elastic relationships can express the decay of elastic modulus E0 at large strain. In appendix A is reported the Tatsuoka and Shibuya (1992) model formulation and the respectively parameters for Ticino sand.

The Poisson coefficient ν can be estimated by the experimental relation: $\nu = 0.15 + 0.45\,f$ where $f = \tau/\tau_{max}$ is a mobilisation factor (Pallara, 1996).

Sand deformability at large strain

The decay of Young's modulus during first loading can be evaluated by means of the following expression (Tatsuoka and Shibuya 1992).

$$\frac{E_s}{E_o} = \frac{y-y_e}{x-x_e} = \frac{1}{\dfrac{1}{C_1(x)} + \dfrac{x-x_e}{C_2(x)}} \quad (B.3)$$

where $y = \dfrac{q-q_o}{q_{max}-q_o}$ is the mobilisation factor; y_e = mobilisation factor at the elastic limit ($y_e = E_o \cdot x_e$); $q = \sigma_1 - \sigma_3$ (deviator stress); $q_o = \sigma_{1o} - \sigma_{3o}$ (deviator stress - end of consolidation); $q_{max} = (\sigma_1 - \sigma_3)_{max}$ (peak deviator stress); $x = \varepsilon_a / (\varepsilon_a)_{RIF}$; $(\varepsilon_a)_{RIF} = \dfrac{q_{max} - q_o}{E_o}$; x_e = normalised elastic limit ($0.00001/\varepsilon_{RIF}$);

$$C_1(x) = \frac{1+C_{1\infty}}{2} + \frac{1-C_{1\infty}}{2} \cdot cos\left[\frac{\pi}{\frac{a}{x}+1}\right] \quad (B.4)$$

$$C_2(x) = \frac{C_{20}+C_{2\infty}}{2} + \frac{C_{20}-C_{2\infty}}{2} \cdot cos\left[\frac{\pi}{\frac{b}{x}+1}\right] \quad (B.5)$$

$C_{1\infty}, C_{20}, C_{2\infty}, a, b$ are model parameters which mainly depend on the stress history (OCR) and consolidation stress ratio $K_c = \sigma'_{hc} / \sigma'_{vc}$.

In the case of soil elements with $K_A < K_c < K_o$ the model parameters take on the values listed in Table B.3 (Pallara, 1996).

Table B.3: Model parameters for quasi-elastic relationships (Pallara, 1996)

	$C_{1\infty}$	C_{20}	$C_{2\infty}$	a	b
NC	0.20	0.08	1	0.2	0.88
OC	0.35	0.85	1	3.0	0.80

The decay curves, which are obtained from cyclic loading tests, indicate a much stiffer response of sand after a certain number of cycles. In this case the consolidation pressure mainly controls the decay. In the case of one-dimensional loading conditions it is quite easy to obtain cyclic stiffness from the skeleton curve using a modified second Masing (1926) rule. The unloading and reloading branches have the same shape as the skeleton curve but have an amplification of the scale equal to 6 instead of 2.

Fig. B.3 illustrates the experimental decay of shear modulus as a function of cyclic shear strain amplitude observed in resonant column results on TIS for different levels of confining pressure. The decay does not depend upon the relative density of the sand.

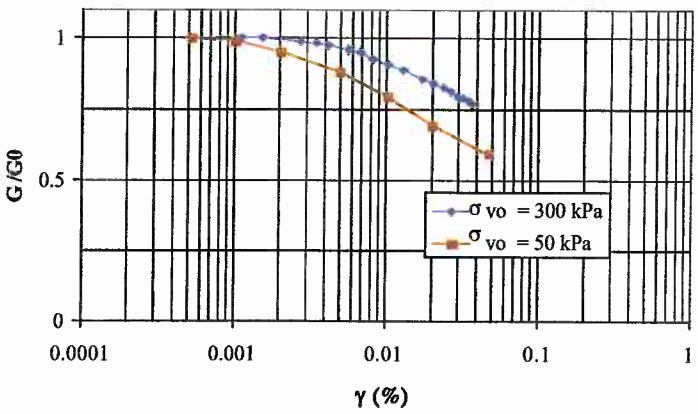

Fig. B.3: Cyclic shear modulus decay of Ticino - Resonant column results

REFERENCES

Bellotti, R., Fretti C., Ghionna V.N. and Pedroni S. (1991) "Crushability of sands in CPT performed in calibration chamber" Proc. IX Asian Regional Conference on SMFE, Bangkok 9-13 Dec. 1991.

Bellotti R., Jamiolkowski M, Lo Presti D.C.F. and D.A. Neill. (1996) "Anisotropy of small strain stiffness in Ticino sand" Geotechnique 46, No.1, pp. 115-131.

Bolton M.D.T, (1986). "The Strength and Dilatancy of Sands", Geotechnique 36, No. 1, 157-164.

Fioravante V., Fretti C., Froio F., Jamiolkowski, M., Lo Presti, D.C.F. and Pedroni S. (1997) "Anisotropy of elastic stiffness in Kenya sand" submitted to Géotechnique for possible pubblication.

Lo Presti D.C.F., Pallara O.› Fioravante V.,and Jamiolkowski M. (1997) "Assessment of quasi-linear models for sands", Geotechnique Symposium in Print, to appear.

Pallara O. (1996) "Verifica delle leggi elastiche quasi-lineari nelle sabbie mediante prove di laboratorio" Rapporto di Ricerca, Aprile 1996, Department of Structural Engineering, Politecnico di Torino, Turin, Italy.

Rondena E. (1984) "Analisi morfologiche della sabbia del Ticino" ENEL CRIS Internal Report

Tatsuoka, F. and Shibuya, S. (1992), "Deformation Characteristics of Soil and Rocks from Field and Laboratory Tests". Keynote Lecture, Proc. IX Asian Conference on SMFE, Bangkok, 1991 2, 101-190.

Mission of the JRC

The mission of the JRC is to provide customer-driven scientific and technical support for the conception, development, implementation and monitoring of EU policies. As a service of the European Commission, the JRC functions as a reference centre of science and technology for the Union. Close to the policy-making process, it serves the common interest of the Member States, while being independent of special interests, whether private or national.

EUROPEAN COMMISSION
JOINT RESEARCH CENTRE